Design Methodology and Optimization of a Medium Frequency Transformer for High Power DC-DC Applications

M. A. Bahmani and T. Thiringer
Chalmers University of Technology
Gothenburg, Sweden
Email: bahmani@chalmers.se
torbjorn.thiringer@chalmers.se

M. Kharezy
SP Technical Research Institute of Sweden
Borås, Sweden
Email: Mohammad.Kharezy@sp.se

***Abstract*—The high power medium frequency transformer (HPMFT) is one of the key elements of an isolated, bi-directional DC-DC converters in applications such as future all-DC offshore wind farms, traction and solid state transformers. This paper describes a design methodology taking into account the loss calculation, isolation requirements and thermal management. Incorporating this design methodology, an optimization process with a wide range of parameter variations is applied on a design example to find the highest power density while the efficiency, isolation, thermal and leakage inductance requirements are all met.**

I. Introduction

Moving towards higher power density in power conversion units has been receiving wide attention over the past decade particularly in highly restricted applications such as wind farm and traction [1], [2]. Operating higher up in frequency is the most common solution to achieve higher power density, because the weight and volume of the magnetic part, the bulkiest element in power electronics converters, are then decreased. However, on the other hand it will lead to higher loss density due to enhanced core loss and more importantly enhanced winding loss [2], [3]. One of the potential applications of the HPMFT is high power isolated DC-DC converters for wind energy DC collection and transmission grids. This could lead to a great weight and size reduction, which is of a particular value for offshore wind installations as stated in [4], in which a 3 MW, 500 Hz transformer is shown to be more than three times lighter than the equivalent 50 Hz one.

Most of the classical attempts for HPMFT designs were focused on a parameter called area product whereby the power handling capability of the core is determined [5], [6]. However, it remains unclear whether this parameter is valid for high power high frequency applications or not [7]. Petkov in [8] presented a more detailed design and optimization procedure of high power high frequency transformers. Some years later, Hurley [9] reported a similar approach accounting for non-sinusoidal excitations. However, the effect of parasitics are essentially neglected in both approaches.

This paper presents a design methodology addressing the high isolation requirements of the off-shore based transformers as well as required leakage inductance of the dual active bridge (DAB) topology as one the most attractive power electronic topologies for high power applications. Incorporating this design methodology, an optimization process with a wide range of parameter variations is performed to get the highest power density while the efficiency, isolation, thermal and leakage inductance requirements are all met [7]. Using the proposed design and optimization methodology, an optimized 1 MW, 3 / 6 kV, 5 kHz medium frequency transformer, to be used in a modular 5 MW turbine based DC-DC converter, is presented as a design example.

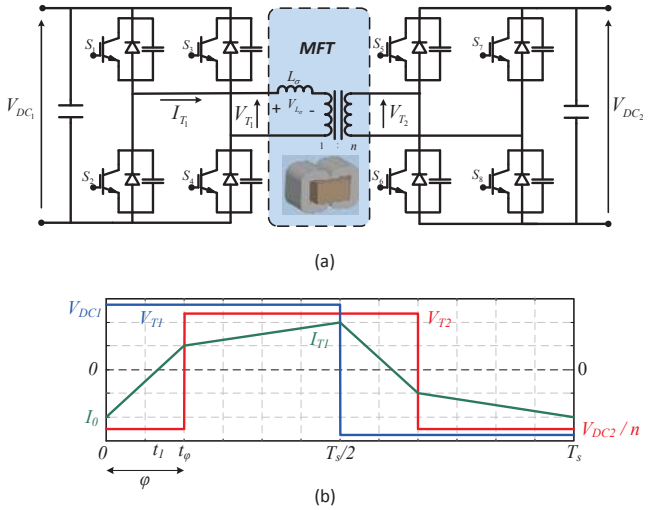

Fig. 1: (a) Dual Active Bridge circuit. (b) Steady state medium frequency transformer voltage and current waveforms

II. DAB Converter

Recently, there has been growing interest in utilizing dual Active bridge (DAB) converters in high power applications. The equivalent circuit of a DAB converter is shown in Fig. 1(a) in which two square wave voltage waveforms on the two sides of the transformer has been shifted by controlling the input and output bridges, applying full voltage over the inductance, L_σ, which is used to shape the current as a power transfer element [10]. The steady state transformer voltage and current waveforms of a DAB converter with simple phase shift modulation are shown in Fig. 1(b). It is worth to point out

that in order to have soft switching at turn on, the anti-parallel diode of each switch should start conducting prior to the turn on moment. In order to achieve zero voltage switching (ZVS) at turn on, the phase shift between the bridges, φ, should be higher than a certain value resulting in a minimum value of the series inductance as presented in (1). This inductance is preferably integrated as the leakage inductance of the medium frequency transformer, Fig. 1(a), in order to reduce the number of components, hence achieving higher power densities.

$$L_\sigma = \frac{V_{DC_1} V_{DC_2} \varphi_{min} (\pi - \varphi_{min})}{2 P_{out} \pi^2 f_s n} \tag{1}$$

where φ_{min} can be calculated by the following conditions

$$\begin{aligned} \varphi &> \frac{\pi\,(d-1)}{2d} \quad for \quad d > 1 \\ \varphi &> \frac{\pi\,(1-d)}{2} \quad for \quad d < 1 \end{aligned} \tag{2}$$

and d is defined as

$$d = \frac{V_{DC2}}{n V_{DC1}}. \tag{3}$$

The waveforms illustrated in Fig. 1(b) will be later, in this paper, used as the transformer excitations and consequently they will affect the transformer losses, i.e, copper and core losses. Using (3), the apparent power of the transformer can be calculated from

$$\begin{aligned} S_T &= \frac{1}{2}\left(V_{T1(rms)} I_{T1(rms)} + V_{T2(rms)} I_{T2(rms)}\right) \\ &= \frac{1}{2} V_{DC1} I_{T1(rms)} (1+d) \end{aligned} \tag{4}$$

III. Optimization Procedure

In contrast to most of the proposed design methodologies for high frequency transformers focusing on core selection based on a parameter called area product, A_p, [5], [11] the design methodology proposed in this article stands for the integrated leakage inductance of the transformer and its corresponding phase shift within the DAB topology. Moreover, the isolation requirements introduced by the medium voltage DC link is considered as one of the design inputs making this design suitable for high power medium frequency off-shore dc-dc converters [7]. Moreover, unlike the conventional design of magnetic components where the core will be initially selected from a manufacturer look-up table, the core dimensions are not a limiting factor in this optimizations [8], [12]. It is assumed that specific core dimensions for specific high power density applications can be tailored by core manufacturers.

Fig. 2 shows the proposed optimization flowchart used for designing a medium frequency high power transformer which is supposed to meet the mentioned requirements. First, the converter level requirements, i.e, output power, voltage levels, operating frequency, transformer turn ratio, required leakage inductance and isolation requirements are selected. Then, fixed parameters including suitable core material selection, inter layer and inter core distances and the insulation material are chosen. Having the dielectric characteristics, the minimum required isolation distance and clearance distances are calculated.

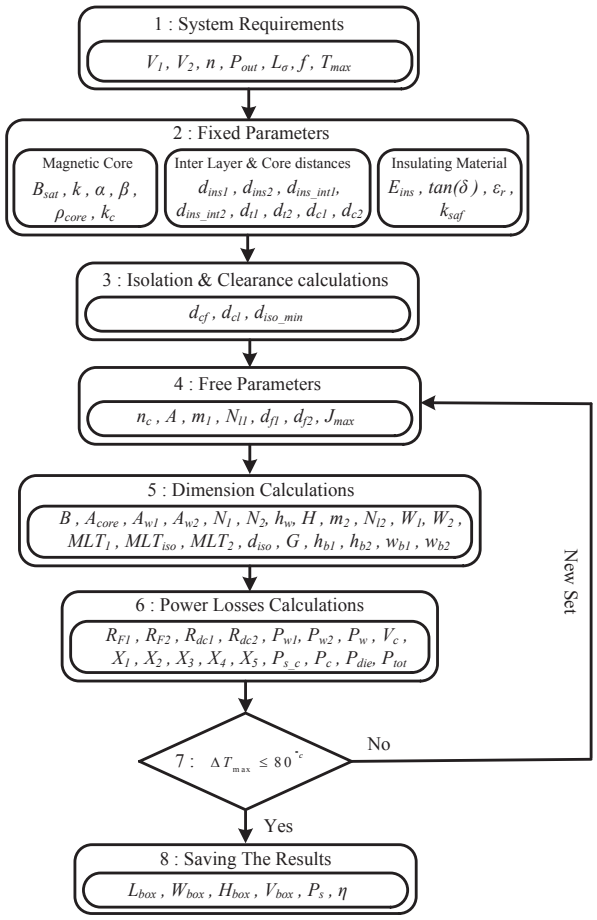

Fig. 2: Design Algorithm.

After selecting the magnetic core material, dielectric material and the required fixed distances, several free parameters composed from geometrical and electrical parameters are chosen and are swept within a wide range in order to find the minimum transformer volume meeting the efficiency and heat dissipation demands. Once a set of free parameters are established, one can determine all the geometrical dimensions of the transformer addressing the required distances to achieve the desirable leakage inductance, winding and core dimensions and other geometrical parameters shown in Fig. 2 and Fig. 3 which illustrates all the frontal, lateral and top dimensions of the desired transformer design.

The next stage is the losses evaluation performed by utilizing the modified empirical methods and FEM derived analytical methods explained in this article. On the other hand the maximum heat dissipation capability of the transformer corresponding to each combination of free parameters are calculated in order to reject those combinations of free parameters which resulted in unacceptable power losses. Finally, the optimal set of free parameters resulting in the highest efficiency while meeting the loss dissipation, isolation and leakage inductance requirements are presented. These steps are

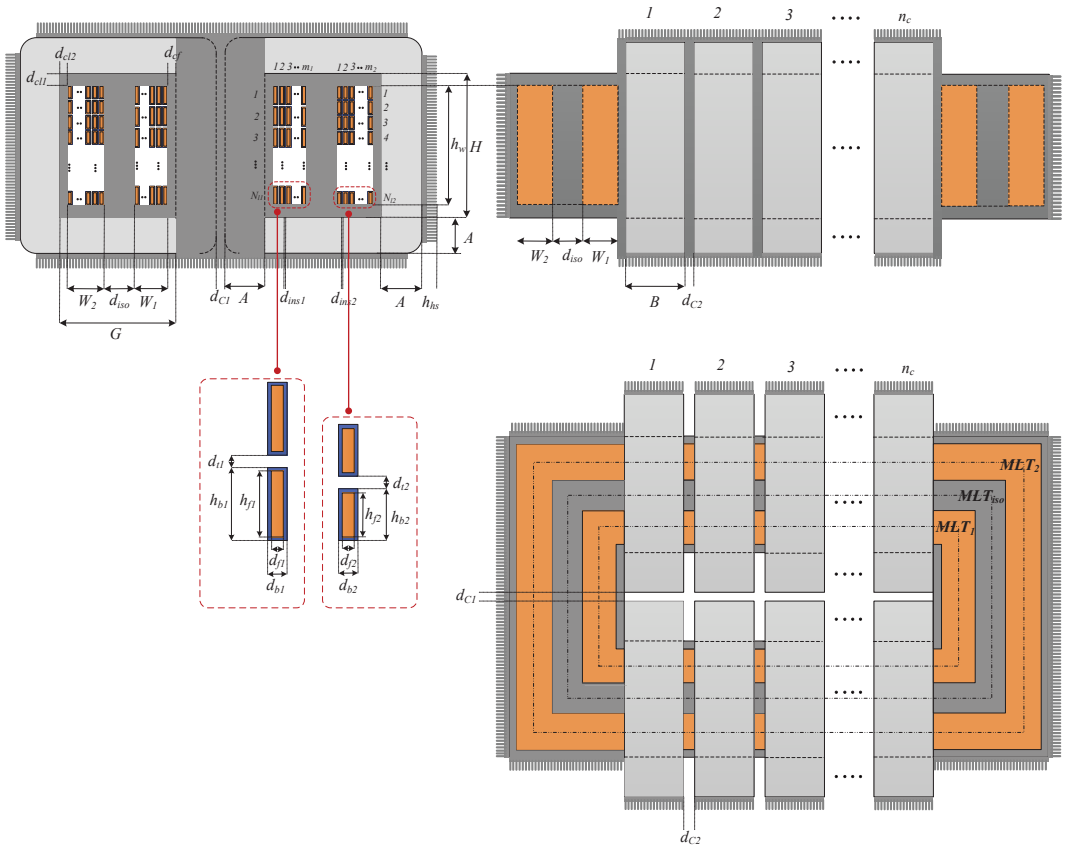

Fig. 3: Design sketch.

described in detail as follows.

A. System Requirements and the Case Study

A 5 MW, 3/30 kV turbine base isolated DC-DC converter has been considered as a case study in this chapter. Similar to the configuration presented in Fig. 4, this converter can be considered as 5 modules connected in parallel at the low voltage side (generator side) and in series at the high voltage side (MVDC link). The specification of each module are tabulated in Table. I. The isolation level, 60 kV, is considered to account for two times of the MVDC voltage level. The designated value of the leakage inductance ensures soft switching of the converter with a maximum of 5% output voltage deviation.

The transformer is exposed to the voltage and current waveforms shown in Fig. 1(b) as the typical waveforms of a DAB converter. However, the proposed design methodology can easily be applied on other types of modulations with duty cycles, D_1 and D_2, being below 0.5.

B. Fixed Parameters

Prior to the iterative part of the optimization, the magnetic core material, insulation material and the windings inter-layer distances need to be set. The favorable magnetic materials for magnetic components in a higher range of frequency and power are the ones with lowest core losses, higher saturation flux densities and higher continuous operating temperature [13]. All these characteristics have to be understood and taken into account in order to have a suitable selection. Among all categories of magnetic materials which are suitable for high frequency applications, ferromagnetic materials are favored to be used in higher power density applications, due to their higher saturation flux densities than ferrites [14]–[16]. Particularly, amorphous and nanocrystalline materials are categorized as low loss and high saturation level ferromagnetic material [17], [18]. Therefore, Vitroperm500F is chosen as the magnetic material used in the current case study optimization. Later, the design outcomes using different magnetic materials are compared in order to observe the effect of different magnetic materials on the efficiencies and power densities.

Insulation material determines the other set of fixed parameters used in the proposed design methodology. As can be seen in Fig. 3, a dry type isolating material, which provides high dielectric strength, is used within the isolation and clearance distances, d_{iso} and d_{cl}. In addition, as shown in Fig. 3, the coil former which provide a distance between the inner layer of the primary windings and the core, d_{cf}, is composed of a casted thermally conductive polymeric material, CoolPoly-D5108, enabling a proper heat conduction to the heat sinks implemented on the core surfaces as well as providing enough isolation between the primary windings and the core [19]. The dielectric and thermal characteristics of some isolating materials, i.e, Dielectric strength, E_{ins}, dielectric constant, ε_r, loss tangent of the dielectric material, $tan\delta$, as well as thermal conductivity of the dielectric medium are presented in Table II.

The third types of the fixed parameters are the inter-layer

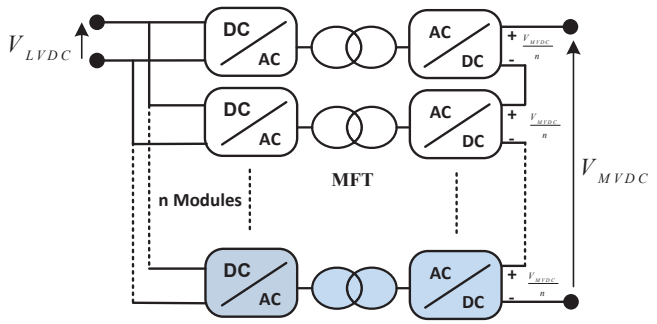

Fig. 4: Parallel input, series output modular configuration of the isolated DAB DC-DC converter for HVDC offshore applications.

TABLE I: Design specification of one converter module

Output Power, P_{out}	1 MW
Module LV side voltage, V_{LV}	3 kV
Module HV side voltage, V_{HV}	6 kV
Leakage inductance, L_σ	22 μH
Transformer turn ratio, n	2
Isolation level, V_{iso}	60 kV
Switching frequency, f	5 kHz

and inter-core distances as well as the outer insulation thickness of the wires used. The horizontal and vertical distances between the wires, d_{ins1}, d_{ins2}, d_{t1} and d_{t1} as shown in Fig. 3. These distances are apart from the outer insulation thickness of the wires which is assumed to be 0.5 mm for the current case study. Moreover, the frontal and lateral distances between the magnetic core stacks are considered to be 1 mm.

C. Free Parameters

For the purpose of this study, 7 free parameters which are swept over a wide range are designated as the number of the magnetic core stacks, n_c, the frontal side of the core cross section, A, the number of layers and the number of turns per layer in primary portion, m_1 and N_{l1}, the effective thickness of the primary and secondary copper foils, d_{f1} and d_{f2} and finally the maximum allowed RMS value of the current density through a conductor, J_{max}. The selection of free parameters highly depends on the optimization targets and restrictions, as well as the considered core and winding topologies. For instance, in case of litz conductors, one can consider the number of strands, strands diameter and the bundle dimensions as complementary free parameters.

All possible combinations of these free parameters will be applied to the optimization flowchart shown in Fig. 2, resulting in distinct transformer geometries corresponding to its set of free variables. Utilizing the modified and developed expressions, the core, windings and dielectric losses are then being evaluated for each set of free parameters [20], [21]. The efficiency, power density and temperature rise of each transformer are then extracted and compared in order to obtain the optimum combination that meets the requirements.

D. Geometry Construction

Having the fixed and free parameters, the transformer geometry can be defined as follows. First, the required magnetic core cross section is defined as

$$A_c = \frac{V_{rms1}}{k_f k_c N_1 B_m f} \tag{5}$$

where V_{rms} is the RMS value of the primary voltage, k_c is the filling factor of the core, N_1 is the number of primary turns, $N_1 = m_1 N_{l1}$, and f is the fundamental frequency. The coefficient k_f is defined as

$$k_f = \frac{2\sqrt{2D - \frac{8}{3}R}}{D - R} \tag{6}$$

where D is the duty cycle and R is the relative rise time in the rectangular waveform with respective rise and fall time defined as

$$D = \frac{t_{on}}{T} \leqslant \frac{1}{2} \quad , \quad R = \frac{t_r}{T} \leqslant \frac{1}{4}. \tag{7}$$

It should be noted that for the phase shift modulation in the DAB converter, the value of D is considered as 0.5 and R equals to zero. Moreover, in order to avoid the core saturation due to unwanted magnetic flux density fluctuation, the maximum induction level, B_m, is considered as 80 % of the saturation level of the selected magnetic core. Hence, considering the geometry structure shown in Fig. 3 and considering the number of core stacks, n_c, the lateral side length of the magnetic core can be calculated as

$$B = \frac{A_c}{2 n_c A} \tag{8}$$

where A is the frontal side length of each core stack. The required clearances can be calculated by

$$d_{cf} = \lceil \frac{V_{LVDC}}{k_{saf} E_{ins}} \rceil \quad , \quad d_{cl1,2} = \lceil \frac{V_{MVDC}}{k_{saf} E_{ins}} \rceil \tag{9}$$

$$d_{iso-min} = \lceil \frac{V_{iso}}{k_{saf} E_{ins}} \rceil \tag{10}$$

where, a safety factor of 30 %, k_{saf}, is considered for the dielectric strength of the isolating medium, resulting in $d_{cf} = 1$ mm, $d_{cl1,2} = 4$ mm and $d_{iso-min} = 7$ mm which is the minimum allowed isolation distance between the primary and secondary windings in order to meet the isolation requirements of 60 kV. However, the actual value of d_{iso} will later be calculated with respect to the desired leakage inductance.

The copper foil heights of the primary and secondary windings are then calculated as

$$h_{b1} = 2 d_{ins-int1} + \frac{I_{T1}}{d_{f1} J_{max}} \tag{11}$$

TABLE II: Electrical and thermal characteristics of some isolation medium [22]–[24]

Dielectric Material	Thermal Conductivity $[\frac{W}{m.K}]$	Dielectric Strength $[\frac{kV}{mm}]$	$tan\delta$	Dielectric Constant ε_r
Air	0.03 (@70°C)	3	0	1.0005
Epoxy resin	0.25	15	0.021 (@ 100kHz)	3.6
CoolPoly-D5108 [19],	10	29	0.022 (@ 100Hz)	4.8
Mica	0.71	11-43	-	2.5-7
Transformer oil	0.12	10-15	2e-6 (@ 50MHz)	2.2-2.5
Paper	0.05	22-49	6e-5 (@ 1kHz)	2.3-5
RTV (Oxime)	1.8	8	-	-
NOMEX	-	27	5e-3(@ 60Hz)	2.5-4

$$h_{b2} = 2d_{ins-int2} + \frac{I_{T1}}{nd_{f2}J_{max}} \tag{12}$$

where I_{T1} is the function of the applied phase shift, φ, which is the minimum allowed value ensuring the soft switching and yet having a reasonable amount of reactive power circulation. Assuming a maximum voltage deviation of 5 % and using (2), the minimum value of φ, ensuring ZVS turn on, is 0.075 rad or 4.3 degree. Thus, I_{T1} can be calculated from

$$I_{T1}\left(rms\right) = Z\sqrt{\frac{4t_1^2t_\varphi + T_st_1^2 - 4t_\varphi^2t_1 - T_st_1t_\varphi + T_st_\varphi^2}{3T_s}} \tag{13}$$

where Z, t_1 and t_φ are respectively calculated by

$$Z = \frac{nV_{DC1} + V_{DC2}}{nL_\sigma} \tag{14}$$

$$t_1 = \frac{\pi + 2\varphi d - \pi d}{4\pi f\left(1+d\right)} \tag{15}$$

$$t_\varphi = \frac{\varphi}{2\pi f}. \tag{16}$$

As a result, the winding height, h_w, the core window height, H, and the primary windings build are respectively calculated as

$$h_w = \left(N_{l1}+1\right)h_{b1} + N_{l1}d_{t1} \tag{17}$$

$$W_1 = m_1\left(d_{f1} + 2d_{ins-int1}\right) + \left(m_1 - 1\right)d_{ins1} \tag{18}$$

$$H = h_w + 2d_{cl}. \tag{19}$$

Likewise, the number of turns and layers at the secondary windings are calculated by

$$N_{l2} = \left\lfloor \frac{h_w - h_{b2}}{h_{b2} + d_{t2}} \right\rfloor \tag{20}$$

$$m_2 = \left\lceil \frac{nm_1N_{l1}}{N_{l2}} \right\rceil. \tag{21}$$

Accordingly, the secondary winding build is calculated from

$$W_2 = m_2\left(d_{f2} + 2d_{ins-int2}\right) + \left(m_2 - 1\right)d_{ins2}. \tag{22}$$

Hence, the mean length turn of the primary windings, MLT_1, which will be later used for the windings loss calculation is obtained from

$$MLT_1 = 2\left(2A + d_{c1} + 4d_{cf} + n_cB + \left(n_c - 1\right)d_{c2} + 2W_1\right) \tag{23}$$

E. Isolation Distance

In order to be able to calculate the rest of the geometrical dimensions, i.e, the core window width, the total length and width of the transformer box and consequently the total volume of the box, one first needs to calculate the required isolation distance, d_{iso}, fulfilling the minimum isolation requirements as well as providing the desired leakage inductance ensuring the ZVS operation of the DC-DC converter.

For this purpose, the analytical expression presented in [21], accounting for the high frequency effect on the leakage inductance value, is rearranged as

$$d_{iso} = \frac{-8k_1 - k_2m_1 + \sqrt{\left(k_2m_1 + 8k_1\right)^2 - 16k_3m_1}}{8m_1} \tag{24}$$

where k_1 to k_3 are constants that can be found in [7]. Thus, the expression in (24) gives the required isolation distance providing the desired leakage inductance as one of the design specification. The obtained value of d_{iso} must withstand the isolation voltage level, V_{iso} as well. Otherwise, the design is not acceptable and the next calculation with a new set of the free parameters is initiated.

Having V_{iso} determined, one can uniquely draw the transformer sketch, shown in Fig. 3, with all the geometrical details. Therefore, it is possible to utilize the loss evaluation methods, in order to calculate the power losses of each transformer corresponding to each set of free parameters.

F. Core Loss Evaluation

In order to evaluate the core losses, the modified expression of the improved generalized Steinmetz equation (IGSE) adopted for non-sinusoidal waveforms has been used as

$$P_{core} = \left(2D - \frac{4\alpha}{\alpha+1}R\right)\frac{2^{\beta}}{(D-R)^{\alpha}}k.k_i f^{\alpha} B_m^{\beta} V_c \rho \quad (25)$$

where D and R are equal to 0.5 and 0 respectively for the standard phase shift DAB converter, ρ is the core density and V_c, is the core volume corresponding to the investigated sets of free parameters as follows

$$V_c = 4n_c A.B\,(H + 2A) + 4n_c A.B.G \quad (26)$$

in which H is the window height previously calculated in (19) and G is the core window width calculated from

$$G = d_{cf} + W_1 + d_{iso} + W_2 + d_{cl} \quad (27)$$

G. Windings Loss Evaluation

To accurately evaluate the winding losses as an essential step in a high power density magnetic design, the pseudo-empirical method developed in [2] has been utilized. On the basis of the fact that copper has linear characteristics, the winding losses can be calculated using the harmonic contents of the applied current, thus

$$P_{w1} = \sum_{h=1}^{n} R_{DC1}.RF_{1_h}.I_{1_h}^2 \quad , \quad P_{w2} = \sum_{h=1}^{n} R_{DC2}.RF_{2_h}.I_{2_h}^2 \quad (28)$$

where R_{DC1} and R_{DC2} are the DC resistance of the primary and secondary windings portion, RF_{1_h} and RF_{2_h} are respectively the AC resistance factor of the primary and secondary windings portion at the h^{th} harmonic, as well as I_{1_h} and I_{2_h}, which are respectively the RMS value of the primary and secondary currents through the transformer windings for the h^{th} harmonic. The DC resistance of the primary and secondary windings portion associated with the winding arrangement in Fig. 3 are calculated from

$$R_{DC1} = \frac{m_1 N_{l1} MLT_1}{\sigma d_{f1} h_{f1}} \quad , \quad R_{DC2} = \frac{m_2 N_{l2} MLT_2}{\sigma d_{f2} h_{f2}} \quad (29)$$

where σ is the conductivity of the conductors, here copper.

1) AC Resistance Factor: As shown in Fig. 1(b), the transformer voltages and currents are not sinusoidal. Therefore, AC resistance factors, RF_{1_h} and RF_{2_h}, should be, separately for each harmonic content, calculated from the expression derived in [2] as

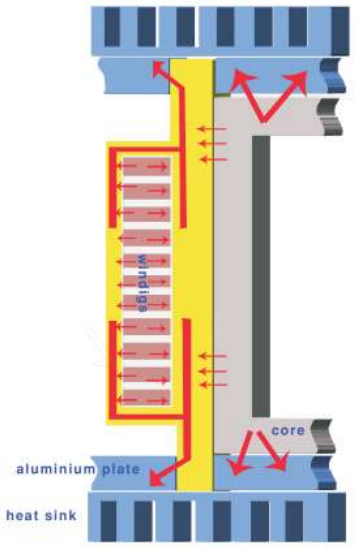

Fig. 5: Thermally conductive, electrically dielectric polymeric coil former (yellow) which extracts the heat from hot spots to the heat sinks.

$$\begin{aligned} RF_h &= f(X_1, X_2, X_3, X_4, X_5) \\ &= \sum_{i=0}^{5}\sum_{j\geq i}^{5}\sum_{m\geq j}^{5}\sum_{n\geq m}^{5}\sum_{s\geq n}^{5}\sum_{t\geq s}^{5} P_{ijmnst}.X_i.X_j.X_m.X_n.X_s.X_t \\ &+ \sum_{m=1}^{3}\sum_{i=0}^{5}\sum_{j\geq i}^{5} P_{ijm}.X_i.X_j.e^{-(X_1.X_2)^m} + \sum_{i=1}^{5} P_i \frac{X_4^2}{(X_1.X_2)^i} \end{aligned} \quad (30)$$

where X_1 to X_5 are five generic dimensionless parameters, defined based on the primary and secondary windings normalized dimensions.

H. Dielectric Loss Evaluation

In low frequency applications, dielectric losses are often negligible, however when operating in higher frequencies, this type of loss are also important to be considered particularly in high power density applications where the design already is pushed to its limits. The dielectric losses are calculated from

$$P_{ins} = \Delta V_{ins}^2 . 2\pi f . C_{ins} . tan(\delta) \quad (31)$$

in which $tan(\delta)$ is the dissipation factor of the dielectric material, already presented in Table. II, C_{ins} and ΔV_{ins} are respectively the capacitance of the dielectric medium and the voltage over it. It should be pointed out that for simplicity, the magnetic field within the isolation distance, d_{iso}, coil former distance, d_{cf}, as well as the clearing distances, d_{cl}, is considered to be uniform.

I. Maximum Power Dissipation Capability

The thermal aspects of a magnetic design is one of the most crucial issues since, in principle, it is the main design limitation, specifying the geometrical boundaries in which the magnetic component can continuously operates without exceeding the critical temperature, as one of the design criteria. Under this scope, a proper thermal management scheme is a key to dissipate the power losses and consequently to achieve higher power densities.

The combination of two thermal management methods, shown in Fig. 5, are implemented in the current design approach. First of all, as in planar transformers, heat sinks are considered to be placed on the core surfaces in order to increase the effective surface area resulting in thermal resistance reduction and consequently higher power dissipation capability of the design. The main drawback of this method, besides increasing the total volume of the transformer box, is that due to the poor thermal contact of the core and the primary windings, the heat around the middle limbs, usually the hottest spot of the transformer, can not easily be conducted to the heat sink. For this reason, a complementary thermal management method has been incorporated placing a thermally conductive material between the primary windings and the core in order to directly conduct the heat to the top and bottom part of the transformer where heat sinks are assembled. As a result, with a negligible increase in transformer total volume, heat can be extracted from the hot spots deep inside the transformer. Copper or aluminum straps are suitable candidates for this purpose due to their relatively high thermal conductivity. However, in the current design methodology, a thermally conductive, electrically dielectric, polymeric material, which simultaneously can be considered both as the heat removal medium and a dielectric bobbin or coil former for the transformer, is used, as can be seen in Fig. 5. In addition, using the polymeric material, the possibility of eddy current losses in copper or aluminum due to an unwanted air gap in the core, is considerably reduced.

In principle, defining the convection coefficients is one of the biggest uncertain parts of any magnetic design, due to many practical factors affecting the heat transfer process. Therefore, it may be hard to justify the use of very elaborated methods for specifying these coefficients [22].

IV. Optimization Results

The proposed design methodology explained in this article has been applied on the transformer specification shown in Table. I. For this purpose, each free parameter is swept over a wide range of inputs resulting in more than 600000 combinations of free parameters. These sets of free parameters are then applied to the design flowchart shown in Fig. 2 to find the optimum set. The optimization outcome showing the efficiencies and power densities of the transformer designs corresponding to accepted sets of free parameters illustrated in Fig. 6. Therefore, each colored dot represents a distinct transformer which met all the design requirements and its color indicates the corresponding temperature rise of that particular transformer.

The design procedure is performed using two different core materials, Vitroperm500F and 3C85, both suitable for high frequency applications. As can be seen in Fig. 6, Vitroperm500F demonstrates higher efficiencies for the same power density which can be explained by the lower specific losses of Vitroperm500F compared to 3C85. Furthermore, Fig. 6 shows that Vitroperm500F can achieve substantially higher power densities of about 25 kW/L with maximum $60°C$ temperature increase compared to the one of about 10 kW/L for 3C85. This also can be explained by the relatively higher saturation level of Vitroperm500F compared to the one of 3C85.

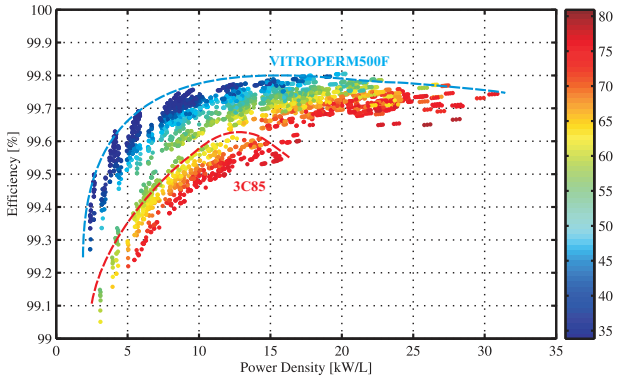

Fig. 6: Efficiency versus Power density of feasible case study transformers according to the proposed design methodology with two different core materials.

It is worth to mention that the high isolation requirements of the case study transformer, 60 kV isolation for a 3/6 kV transformer, together with the desired leakage inductance as the design inputs, play an important role in determining the power density of the final optimum design. Geometrical and electrical characteristics of one of the optimized 1 MW transformer on the pareto-front of the Vitroperm500F in Fig. 6 are summarized in table. III.

As can be seen in table. III, using the design methodology proposed in this chapter, a 1 MW, 3/6 kV transformer operating at 5 kHz can be as compact as 45 liters while the efficiency is about 99.7% and the maximum temperature rise considering natural cooling is $60°C$.

V. Conclusion

The proposed design methodology was applied on a 1 MW case study transformer and the pareto fronts of the power density versus efficiency considering the maximum temperature increase for two different magnetic core materials were studied. The results indicate that such a transformer can achieve the efficiencies as high as 99.74% and the power densities of about 22 kW/L which is substantially higher than the one of the line frequency transformers with similar range of power and voltages.

Acknowledgment

Thanks to the Swedish Energy Agency for the financial support of this research. The authors would also like to thank Dr. Tarik Abdolahovic for his contribution to the project.

TABLE III: Optimal transformer characteristics

Geometrical		Electrical/Magnetic	
Total length	288 mm	Winding losses	1639 W
Total width	335 mm	Core losses	979 W
Total height	542 mm	Dielectric losses	19.5 W
Volume	44.78 Liter	Total losses	2637.5 W
N_1	12	Efficiency	99.74%
N_2	24	Power density	22.33 kW/L
A	40 mm	B_{max}	0.96 T
Isolation distance, d_{iso}	48 mm	J_{max}	3 A/mm2
d_{f1}	1.25 mm	Temperature rise	$59.9^{\circ}C$
d_{f2}	0.5 mm	h_{conv}	3.74
Number of core stacks	3	h_{rad}	6.93

REFERENCES

[1] D. Dujic, F. Kieferndorf, F. Canales, and U. Drofenik, "Power electronic traction transformer technology," in *Power Electronics and Motion Control Conference (IPEMC), 2012 7th International*, vol. 1, june 2012, pp. 636 –642.

[2] M. A. Bahmani, T. Thiringer, and H. Ortega, "An accurate pseudoempirical model of winding loss calculation in hf foil and round conductors in switchmode magnetics," *Power Electronics, IEEE Transactions on*, vol. 29, no. 8, pp. 4231–4246, Aug 2014.

[3] R. T. Naayagi, A. Forsyth, and R. Shuttleworth, "High-power bidirectional dc-dc converter for aerospace applications," *Power Electronics, IEEE Transactions on*, vol. 27, no. 11, pp. 4366–4379, 2012.

[4] S. Meier, T. Kjellqvist, S. Norrga, and H.-P. Nee, "Design considerations for medium-frequency power transformers in offshore wind farms," in *Power Electronics and Applications, 2009. EPE '09. 13th European Conference on*, Sept 2009, pp. 1–12.

[5] W. Colonel and K. T. McLyman, *Transformer and Inductor Design Handbook, Fourth Edition*. CRC Press, 2011.

[6] S. Farhangi and A. Akmal, "A simple and efficient optimization routine for design of high frequency power transformers," in *Proceeding of 9th EPE Conference*, Sep 1999.

[7] M. A. Bahmani, "Design and optimization of hf transformers for high power dc-dc applications," Licentiate Thesis, Chalmers University of Technology, Gothenburg, Sweden, April 2014.

[8] R. Petkov, "Optimum design of a high-power, high-frequency transformer," *Power Electronics, IEEE Transactions on*, vol. 11, no. 1, pp. 33–42, Jan 1996.

[9] W. Hurley and W. Wolfe, *Transformers and Inductors For Power Electronics, Theory, Design and Applications, First Edition*. John Wiley Sons Ltd, 2013.

[10] R. De Doncker, D. Divan, and M. Kheraluwala, "A three-phase soft-switched high-power-density dc/dc converter for high-power applications," *Industry Applications, IEEE Transactions on*, vol. 27, no. 1, pp. 63–73, 1991.

[11] S. Farhangi and A. Akmal, "A simple and efficient optimization routine for design of high frequency power transformers," in *Proceeding of 9th EPE Conference*, Sep 1999.

[12] M. Mohan, T. Undeland, and W. Robbins, *Power Electronics Converters, Applications, And Design, Third Edition*. John Wiley Sons, Inc, 2003.

[13] W. Shen, F. Wang, D. Boroyevich, and C. Tipton, "Loss characterization and calculation of nanocrystalline cores for high-frequency magnetics applications," *Power Electronics, IEEE Transactions on*, vol. 23, no. 1, pp. 475–484, Jan 2008.

[14] M. Rylko, K. Hartnett, J. Hayes, and M. Egan, "Magnetic material selection for high power high frequency inductors in dc-dc converters," in *Applied Power Electronics Conference and Exposition, 2009. APEC 2009. Twenty-Fourth Annual IEEE*, Feb 2009, pp. 2043–2049.

[15] B. Lyons, J. Hayes, and M. Egan, "Magnetic material comparisons for high-current inductors in low-medium frequency dc-dc converters," in *Applied Power Electronics Conference, APEC 2007 - Twenty Second Annual IEEE*, Feb 2007, pp. 71–77.

[16] Y. Han, G. Cheung, A. Li, C. Sullivan, and D. Perreault, "Evaluation of magnetic materials for very high frequency power applications," in *Power Electronics Specialists Conference, 2008. PESC 2008. IEEE*, June 2008, pp. 4270–4276.

[17] M. A. Bahmani, E. Agheb, T. Thiringer, H. K. Hoidalen, and Y. Serdyuk, "Core loss behavior in high frequency high power transformers—i: Effect of core topology," *Journal of Renewable and Sustainable Energy*, vol. 4, no. 3, p. 033112, 2012.

[18] M. Wasekura, C.-M. Wang, Y. Maeda, and R. Lorenz, "A transient core loss calculation algorithm for soft magnetic composite material," in *Energy Conversion Congress and Exposition (ECCE), 2013 IEEE*, 2013, pp. 3719–3725.

[19] [Online]. Available: http://www.coolpolymers.com/

[20] E. Agheb, M. A. Bahmani, H. K. Hoidalen, and T. Thiringer, "Core loss behavior in high frequency high power transformers—ii: Arbitrary excitation," *Journal of Renewable and Sustainable Energy*, vol. 4, no. 3, p. 033113, 2012.

[21] M. A. Bahmani and T. Thiringer, "Accurate evaluation of leakage inductance in high frequency transformers using an improved frequency-dependent expression," *Power Electronics, IEEE Transactions on*, vol. PP, no. 99, pp. 1–1, 2014.

[22] A. Bossche and V. Valchev, *Inductors and Transformers for Power Electronics, Taylor and Francis Group*. CRC Press, 2005.

[23] [Online]. Available: http://www.kayelaby.npl.co.uk/general_physics/2_6/2_6_5.html

[24] [Online]. Available: http://www.rfcafe.com/references/electrical/dielectric-constants-strengths.htm